

Supplement of

Relationship between latent and radiative heating fields of Tropical cloud systems using synergistic satellite observations

Xiaoting Chen¹, Claudia J. Stubenrauch¹, and Giulio Mandorli¹

¹Laboratoire de Météorologie Dynamique/Institut Pierre-Simon Laplace, (LMD/IPSL), Sorbonne Université, Ecole Polytechnique, CNRS, Paris, France

Correspondence: Xiaoting Chen (xiaoting.chen@lmd.ipsl.fr)

1 Data, Methods and Evaluation

1.1 Artificial Neural Network predictions and evaluation

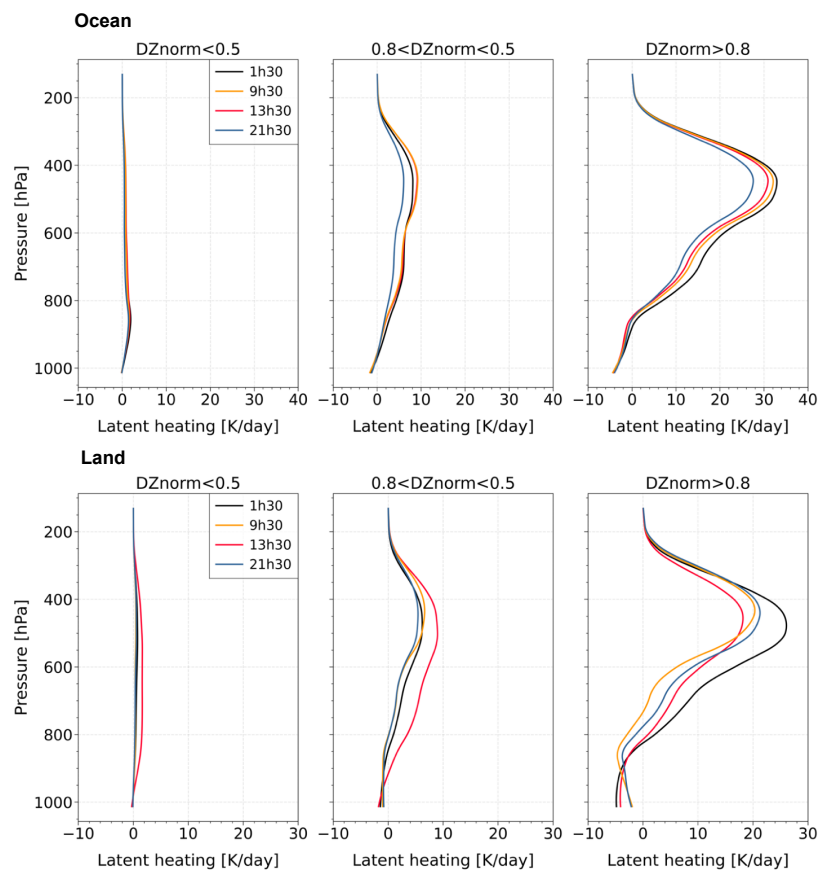


Figure S1. LH profiles of UT clouds, categorized by normalized vertical extent (<0.5 , $0.5-0.8$, >0.8), at 4 observation times (1h30, 9h30 AM/PM), over ocean (top panels) and over land (bottom panels), from the TRMM-SLH retrieval (Shige et al., 2004, 2007, 2008) averaged over the TRMM-CIRS collocated data during the period 2008-2013, within $30^{\circ}\text{N}-30^{\circ}\text{S}$, at a spatial resolution of 0.5° .

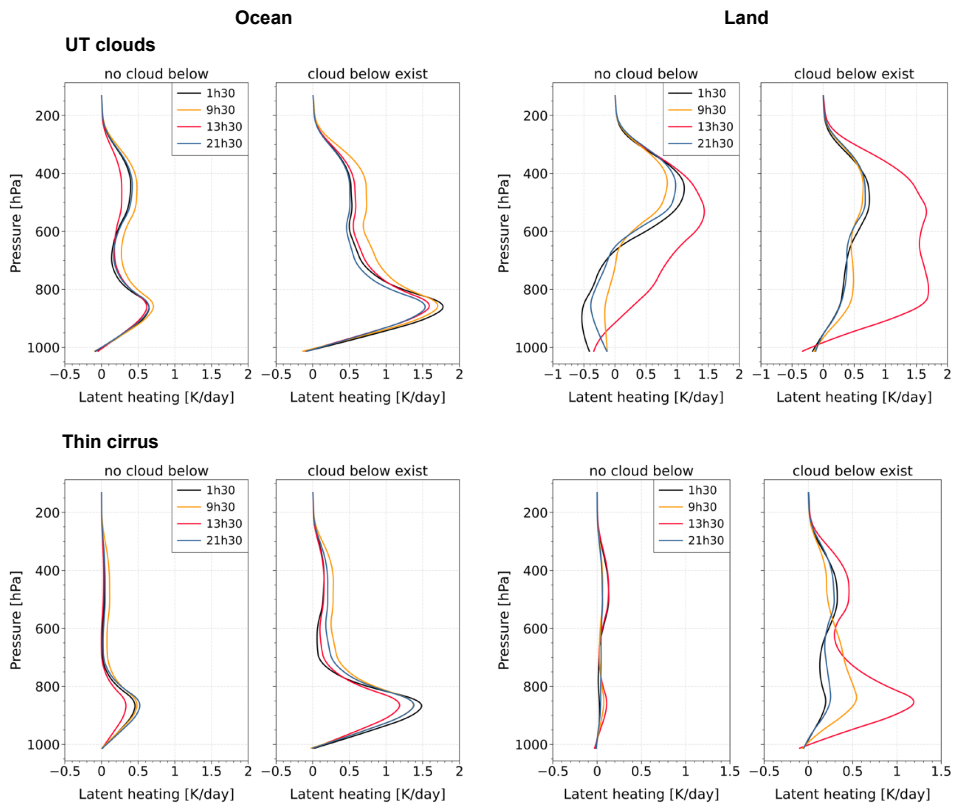


Figure S2. LH profiles of non-precipitating UT clouds (top panels) and thin Cirrus (bottom panels) at 4 observation times (1h30, 9h30 AM/PM), considering the absence or presence of underlying lower clouds (no cloud below, cloud below), separately over ocean (left) and over land (right). Data are from the TRMM–SLH retrieval (Shige et al., 2004, 2007, 2008) averaged over the TRMM–CIRS collocated data during the period 2008–2013, within 30°N – 30°S , at a spatial resolution of 0.5° .

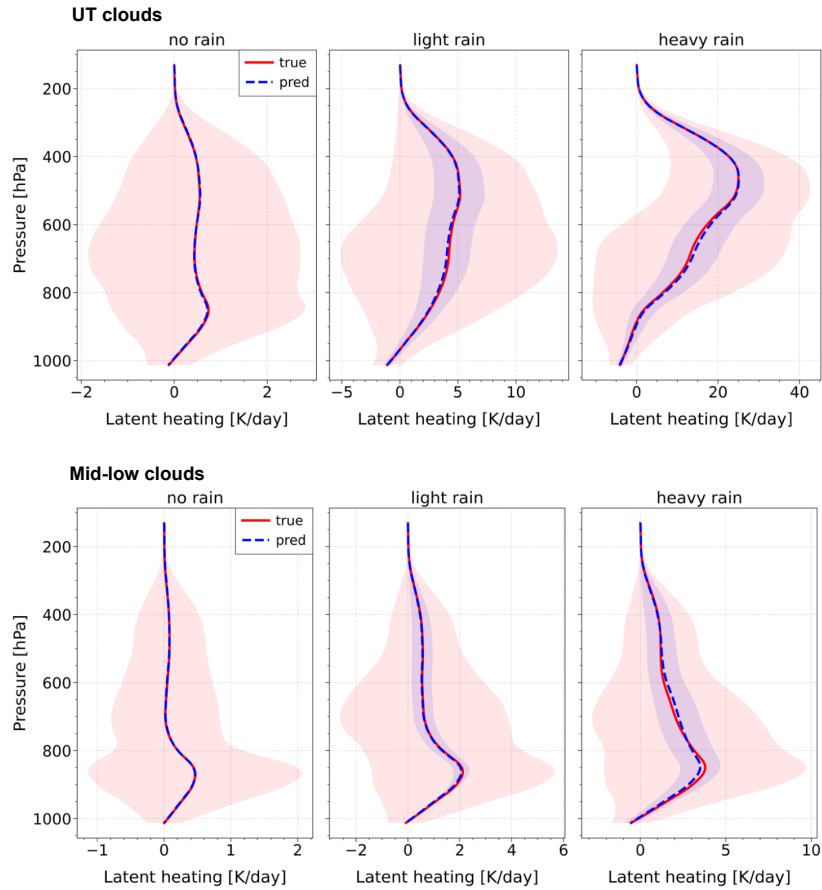


Figure S3. Comparison between predicted (dashed) and observed (solid) LH rates (2004–2013) of UT clouds (top panels, same as the upper panels of Fig. 3, but with independent X-axis tick labels) and mid-low level clouds (bottom panels), for different rain rate intensities (no rain, light rain and heavy rain) over both ocean and land, within 30°N – 30°S , with a spatial resolution of 0.5° . Models were trained on collocated AIRS–TRMM. Shaded areas indicate $\pm 67.5\%$ of the standard deviation, which corresponds to quartiles.

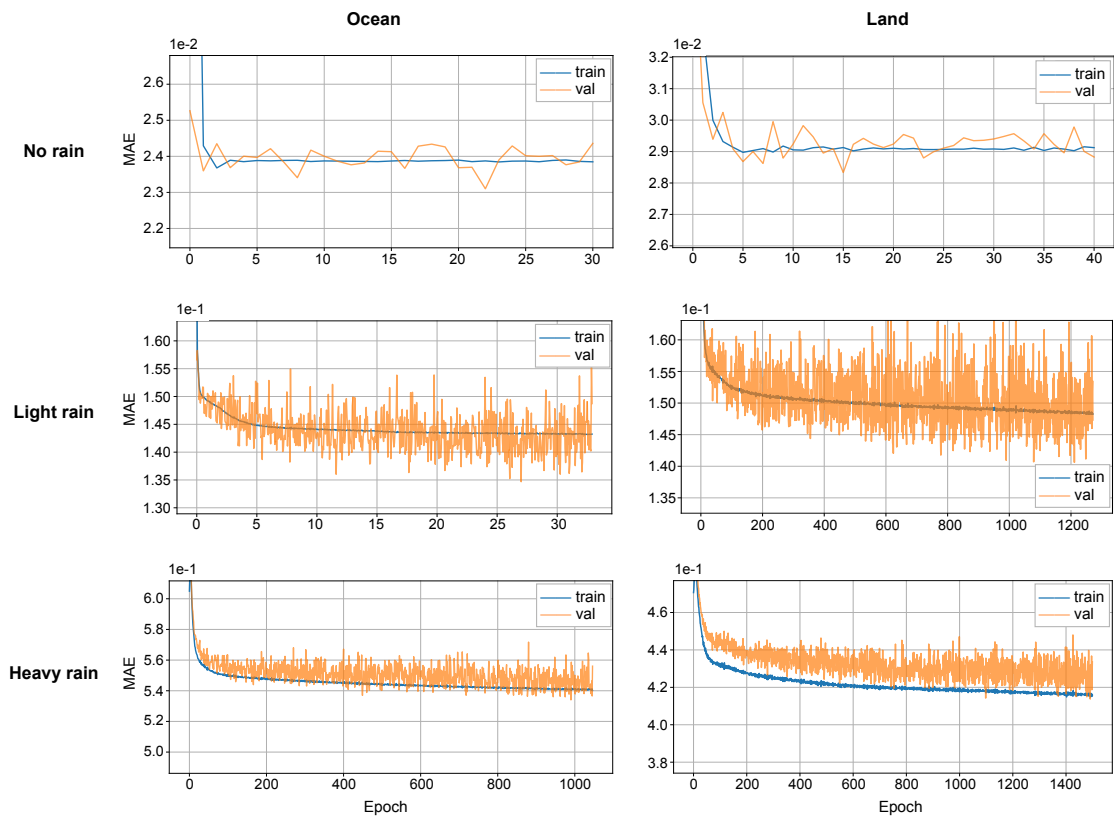


Figure S4. Mean absolute error (MAE) as a function of iterations (epochs) for UT clouds, categorized by three rain intensities (top to bottom: no rain, light rain, heavy rain) over ocean (left) and land (right). ANN regressions were trained on collocated AIRS–TRMM data.

Figure S5 (UT clouds) shows that AIRS has higher LH values at lower altitudes (below 500 hPa) for both true and predicted data compared to IASI over the ocean. Conversely, at higher altitudes, the situation is reversed. This difference is more noticeable over land (Fig. S5b). Below 450 hPa, there is a significant difference between the LH values from AIRS and IASI, and this may be due to the diurnal cycle of precipitation. Another noteworthy point is that the predicted mean demonstrates better performance over the ocean compared to its performance over land, which can be explained by the fact that the ocean surface is more homogeneous. This pattern is also evident in mid-low clouds (Fig. S6).

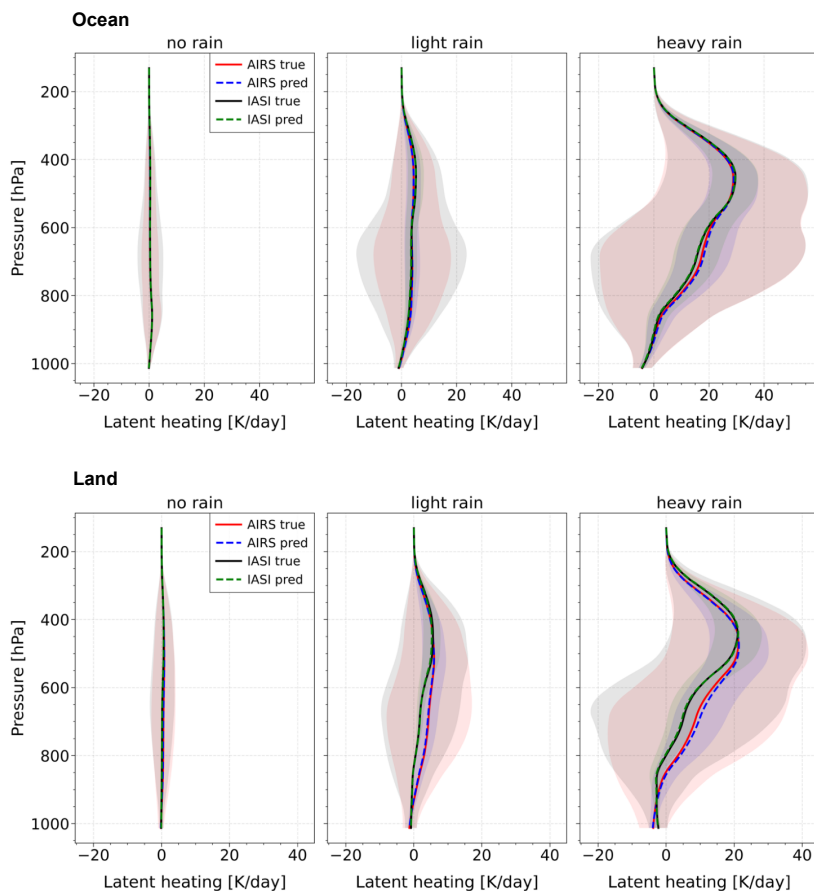


Figure S5. Comparison between predicted and observed LH rates for UT clouds with different rain intensities (no rain, light rain and heavy rain), over ocean (top panels) and land (bottom panels), separately for AIRS and IASI, within 30°N – 30°S , at a spatial resolution of 0.5° . Models were trained on collocated AIRS–TRMM and IASI–TRMM. Shaded areas indicate $\pm 67.5\%$ of the standard deviation, which corresponds to quartiles.

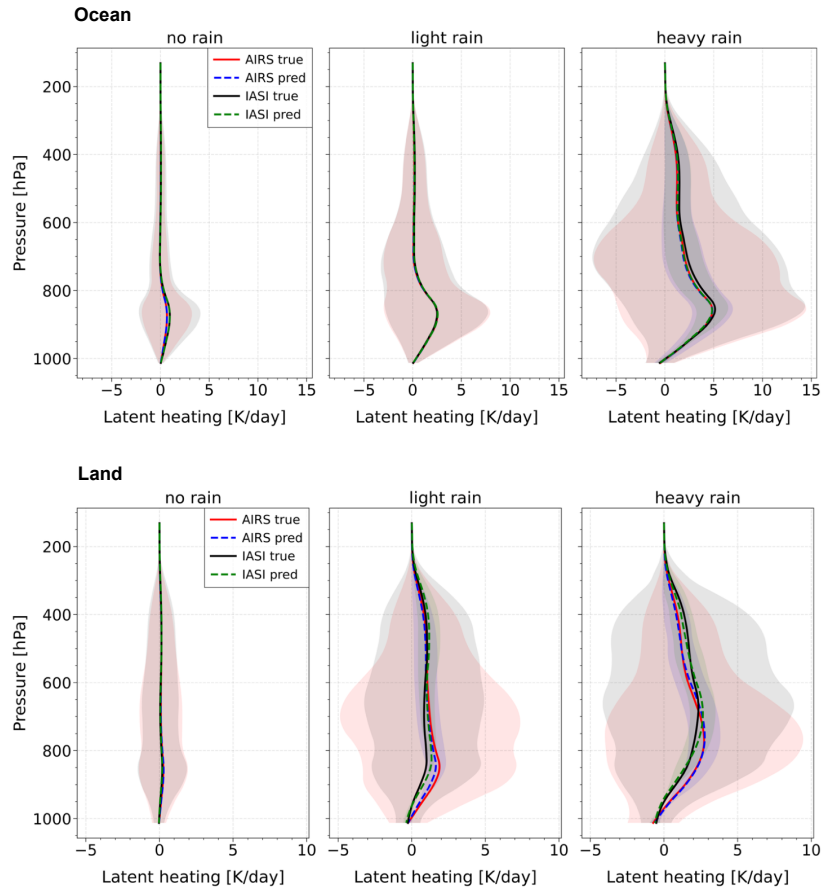


Figure S6. Comparison between predicted and observed LH rates for mid-low level clouds with different rain intensities (no rain, light rain and heavy rain), over ocean (top panels) and land (bottom panels), separately for AIRS and IASI, within 30°N – 30°S , at a spatial resolution of 0.5° . Models were trained on collocated AIRS–TRMM and IASI–TRMM. Shaded areas indicate $\pm 67.5\%$ of the standard deviation, which corresponds to quartiles.

Table S1. Validation MAE (K day^{-1}) for the prediction of LH rates using models over different rain intensity classes.

Scene	Ocean / Land	No Rain	Light Rain	Heavy Rain
AIRS				
UT clouds	ocean	0.024	0.146	0.552
	land	0.029	0.150	0.427
mid-low clouds	ocean	0.008	0.032	0.085
	land	0.008	0.042	0.058
IASI				
UT clouds	ocean	0.027	0.158	0.541
	land	0.022	0.138	0.387
mid-low clouds	ocean	0.012	0.033	0.089
	land	0.007	0.043	0.065

2 Reinforcement of latent heating by UT cloud radiative heating

10 2.1 Relationship between ACRE, LP and environment

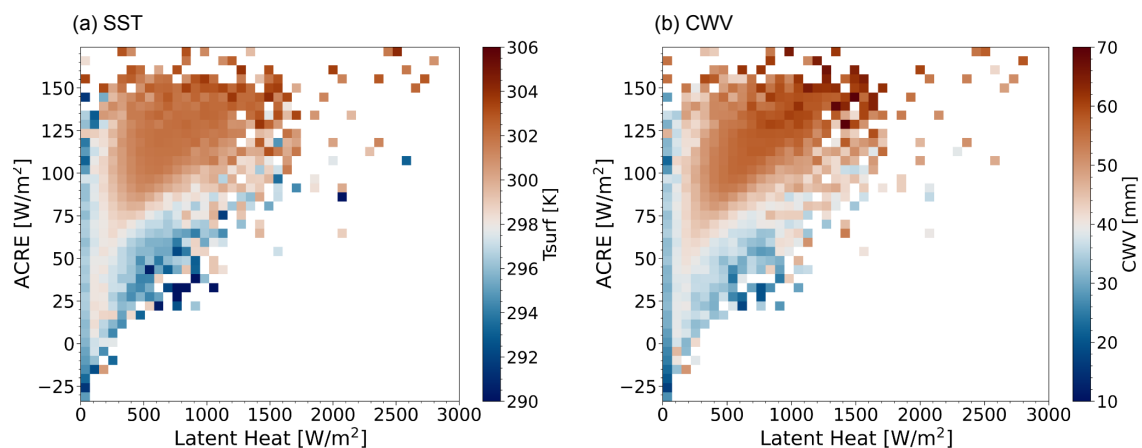


Figure S7. Averages of (a) SST and (b) CWV as function of LP and ACRE released by precipitating UT clouds over the ocean, for the period 2004–2013, spanning 30°N to 30°S, at a spatial resolution of 5°. LP and ACRE are from CIRS–ML, while SST and CWV are from ERA-Interim at 1:30 AM/PM local time. Each square corresponds to a specific LP–ACRE interval.

References

- Shige, S., Takayabu, Y. N., Tao, W.-K., and Johnson, D. E.: Spectral retrieval of latent heating profiles from TRMM PR data. Part I: Development of a model-based algorithm, *Journal of applied meteorology*, 43, 1095–1113, [https://doi.org/10.1175/1520-0450\(2004\)043<1095:SROLHP>2.0.CO;2](https://doi.org/10.1175/1520-0450(2004)043<1095:SROLHP>2.0.CO;2), 2004.
- 15 Shige, S., Takayabu, Y. N., Tao, W.-K., and Shie, C.-L.: Spectral retrieval of latent heating profiles from TRMM PR data. Part II: Algorithm improvement and heating estimates over tropical ocean regions, *Journal of applied Meteorology and Climatology*, 46, 1098–1124, <https://doi.org/10.1175/JAM2510.1>, 2007.
- Shige, S., Takayabu, Y. N., and Tao, W.-K.: Spectral retrieval of latent heating profiles from TRMM PR data. Part III: Estimating apparent moisture sink profiles over tropical oceans, *Journal of applied meteorology and climatology*, 47, 620–640,
- 20 <https://doi.org/10.1175/2007JAMC1738.1>, 2008.